Supplementary Material 2: Setup and results of a model with more geological units

Meshing

To test the sensitivity of the results on the consideration of a higher complexity in terms of geological units, we have built a second mesh (Fig. B1). In this mesh the Cenozoic sediments were divided into Quaternary and Tertiary, and the Pre-Keuper sediments into Muschelkalk, Buntsandstein and Permocarboniferous (Tab. B1). Thus, the mesh differentiates 6 sedimentary units, 3 upper crustal domains and the 2 main border faults. In addition, it includes also the sediments outside the URG (Fig. B1, B2).

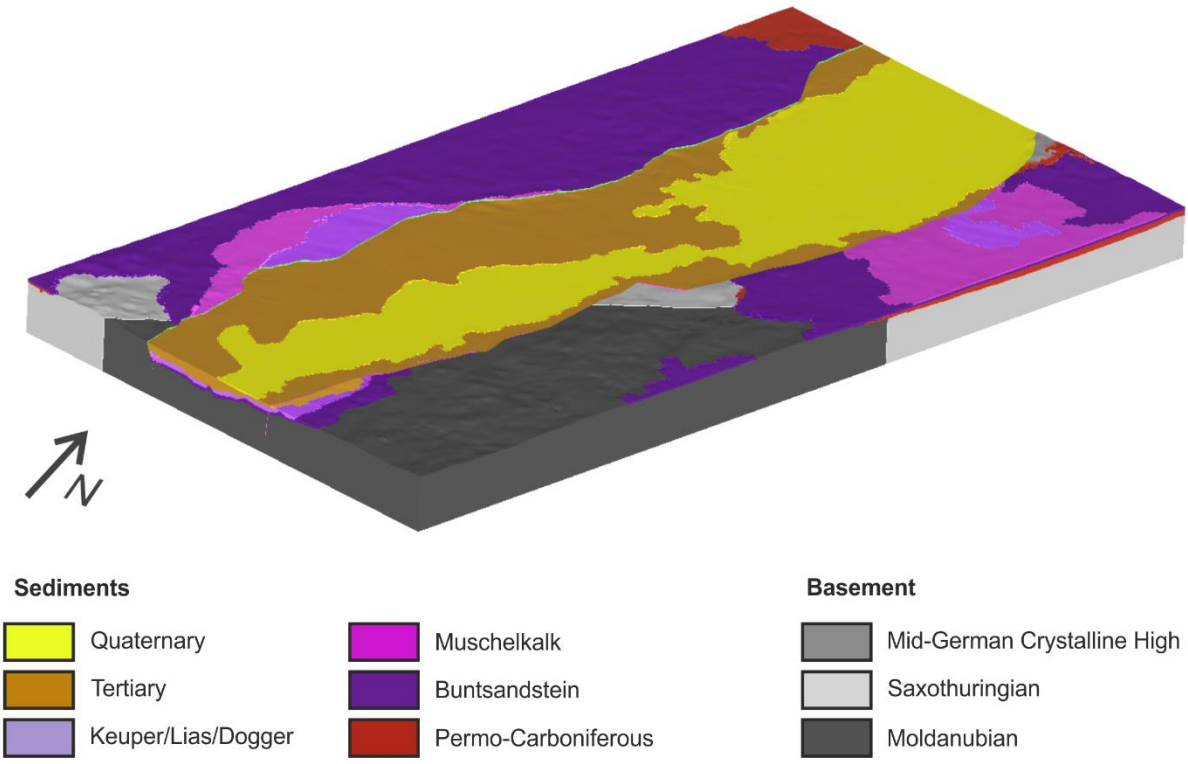

Fig. B1: 3D finite element mesh of the more complex model

The more complex model was meshed with the software Hypermesh (©Altair) and integrates different element types such as tetrahedrons, wedge elements or brick elements. Hypermesh allowed us to integrate out-pinching and outcropping layers like the Keuper/Lias/Dogger-unit in the northern URG

and all sedimentary units outside the URG. However, for technical and numerical reasons minimum thickness for all layers is 100 m. Parts with less than this 100 m were neglected, so that steps were created in the mesh and outcropping layers have a smaller horizontal distribution.

The model area as well as boundary conditions were the same as in the basic mesh described in the main part of this publication.

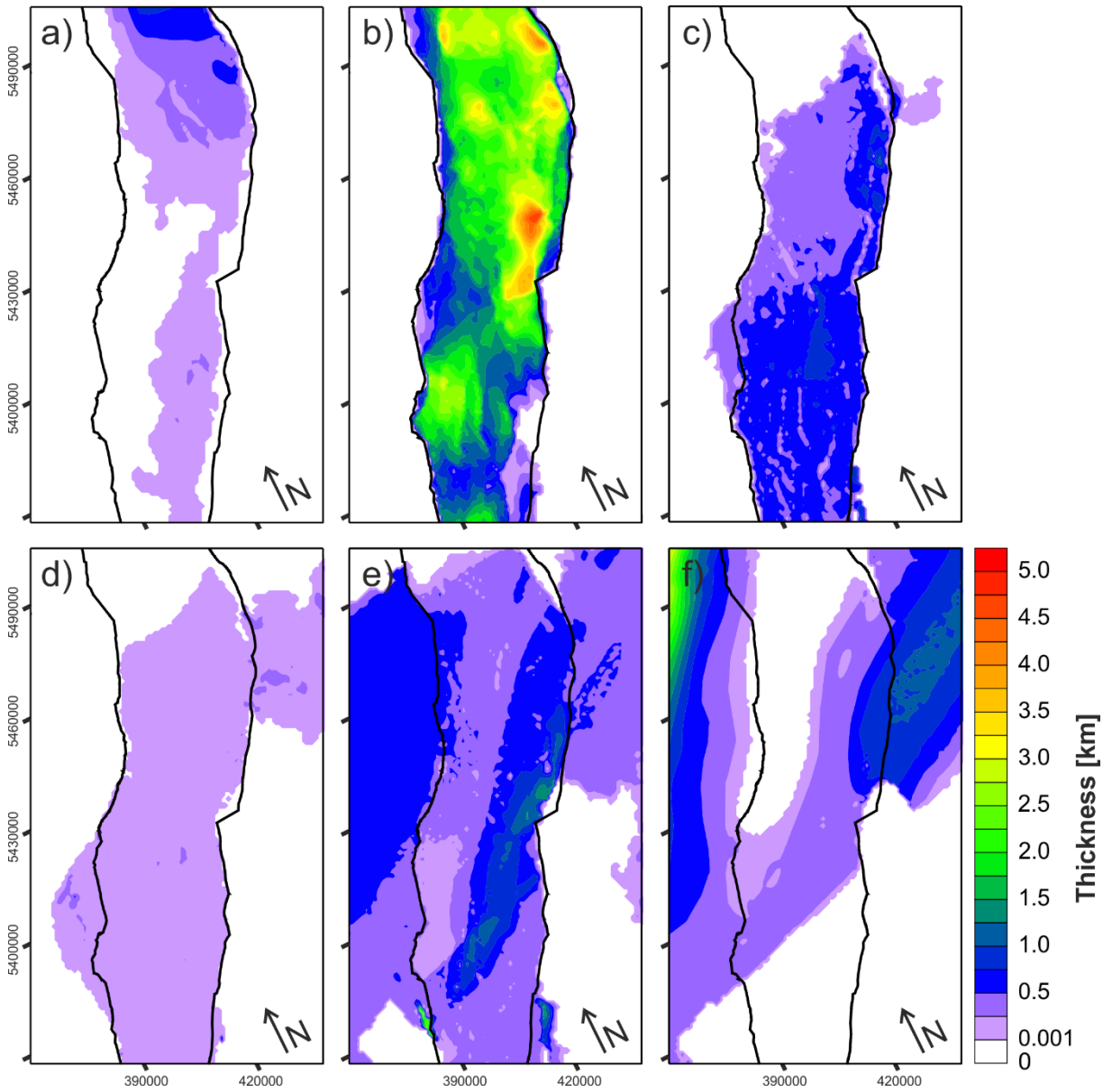

Fig. B2: Thickness of (a) Quaternary, (b) Tertiary, (c) Keuper/Lias/Dogger, (d) Muschelkalk, (e) Buntsandstein and (f) PermoCarboniferous sediments in the more complex model. Maps are shown in UTM32N and rotated counter-clockwise by approximately 20°.

Model Layers and Parameterization

The more complex model differentiates more sedimentary units than the model described in the main part. The Cenozoic sediments are divided into Quaternary sandy gravel and Tertiary marls and sands based on the GeORG model (GeORG-Projektteam 2013a). The Quaternary thickens significantly towards the “Heidelberger Loch” (compare Fig. 3) in the north with a maximum thickness of 780 m (Fig, B2a). It has a high permeability and contains the upper groundwater reservoir (Tab. B1). However, most of the Cenozoic is made up by the Tertiary sands and marls that have a thickness of up to 4700 m (Fig. B2b).

The Dogger/Lias/Keuper unit is pinching out towards the North and has small occurrences in the NE and the SW of the URG (Fig. B2c; compare with Fig. 3b).

The Pre-Keuper sediments were differentiated into Muschelkalk, Buntsandstein and PermoCarboniferous and cover the basement also outside the URG (according to Freymark et al., 2017). Muschelkalk carbonates have an average thickness of 200 m and occur mainly inside the URG (Fig. B2d). Buntsandstein sandstones cover almost the whole model area with an average of 700 m (Fig. B2e). PermoCarboniferous sediments occur only locally inside the URG (Fig. B2f). Highest thicknesses of 3000 m are located in the northwesternmost model area. The crystalline basement is structured in the same way as in the simpler model (Fig. B3).

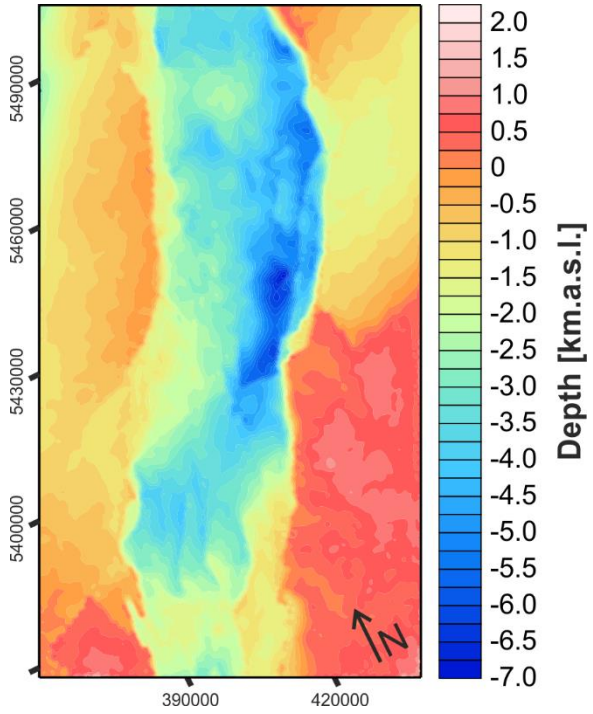

Fig. B3: Depth of top basement of the more complex model. Map is shown in UTM32N and rotated counter-clockwise by approximately 20°.

The parameters used for the coupled thermo-hydraulic simulation are listed in Table B1. The main border faults were parameterized with a width of 1 m and a permeability of 5E-14 m² (to be comparable to model B).

Table B1: Parameter values used for the coupled thermo-hydraulic simulations with the more complex model (UC = upper crust; 1: GeORG-Projektteam 2013a, 2: Bär 2012, 3: Stein 2001, 4: Berger et al. 2011, 5: Altherr et al. 2000, 6: Haenel 1983, 7: Krohe & Eisbacher 1988, 8: GeORG-Projektteam 2013c, 9: Lampe & Person 2002, 10: Bär 2012, 11: Clauser & Villinger 1990, 12: Jodocy & Stober 2011, 13: GeORG-Projektteam 2013b, 14: Stober & Bucher 2015, 15: Stober & Jodocy 2009, 16: Guillou-Frottier et al. 2013, 17: Baujard et al. 2017, 18: Stober & Bucher 2013, 19: Jorand et al. 2015, 20: Dezayes et al. 2008, 21: Surma & Geraud 2003, 22: Wilhelm et al. 1989, 23: Landolt-Börnstein 1982, 24: Gutscher 1991, 25: Freymark et al. 2017)

Layer	Prevailing Lithology	Matrix Porosity	Matrix Permeability [m²]	Specific Heat Capacity [J/(kgK)]	Matrix Thermal Conductivity [W/(m*K)]	Radiogenic Heat Production [µW/m³]	Matrix Density [kg/m³]
Quaternary	Sandy gravel [1]	0.35 [8,9]	1E-12 [9]	850 [18]	1.5 [13]	1.0 [8]	3000 [24]
Tertiary	Marl, sand [1]	0.18 [1,8,9,10,11, 12]	7E-14 [1,9,10,11,12, 14]	860 [19]	1.3 [13]	1.0 [8]	2585 [25]
Dogger/Lias /Keuper	Clay, marl-, lime-, sandstone [1]	0.04 [1]	4E-16 [1,12]	800 [8,18]	2.6 [13]	1.6 [8]	2667 [25]
Muschel-kalk	Carbonates [1]	0.05 [12]	6E-14 [1,10,13,15]	730 [8]	2.1 [10]	1.2 [8]	2863 [25]
Buntsand-stein	Sandstone [1]	0.10 [1,12]	3E-14 [1, 10,14,15,16]	710 [20]	3.3 [13]	1.0 [8]	2778 [25]
Permo-Carbonif-erous	Sandstone, conglomerates, rhyolites [1]	0.07 [9,10, 13]	2E-15 [13]	760 [10]	2.3 [10]	1.0 [8]	2720 [25]
UC: Mid-German Crystalline High	Granitoids [2,3]	0.01 [8]	3E-18 [1]	755 [10]	2.4 [10]	1.8 [6]	2717 [25]
UC: Saxo-thuringian	Slate, granitoids [4,5]	0.01 [8]	3E-18 [1]	900 [8]	2.5 [21]	2.5 [4]	2747 [25]
UC: Mold-anubian	Gneiss, granitoids [6,7]	0.01 [8]	3E-18 [1]	900 [8]	2.5 [22]	2.6 [23]	2707 [25]

Results and Discussion

The basin-wide fluid flow in the URG (Fig. A4) shows the same main characteristics than in the simpler model (Fig. 7). Differences in fluid velocities are most obvious outside the URG, where the complex mesh differentiates high-permeable sediments from low-permeable crystalline crust. Local differences in fluid velocities and minor changes in fluid direction inside the URG can be explained by the differentiation of more sedimentary units and thus more variations in permeability (compare also Table 3 and B2).

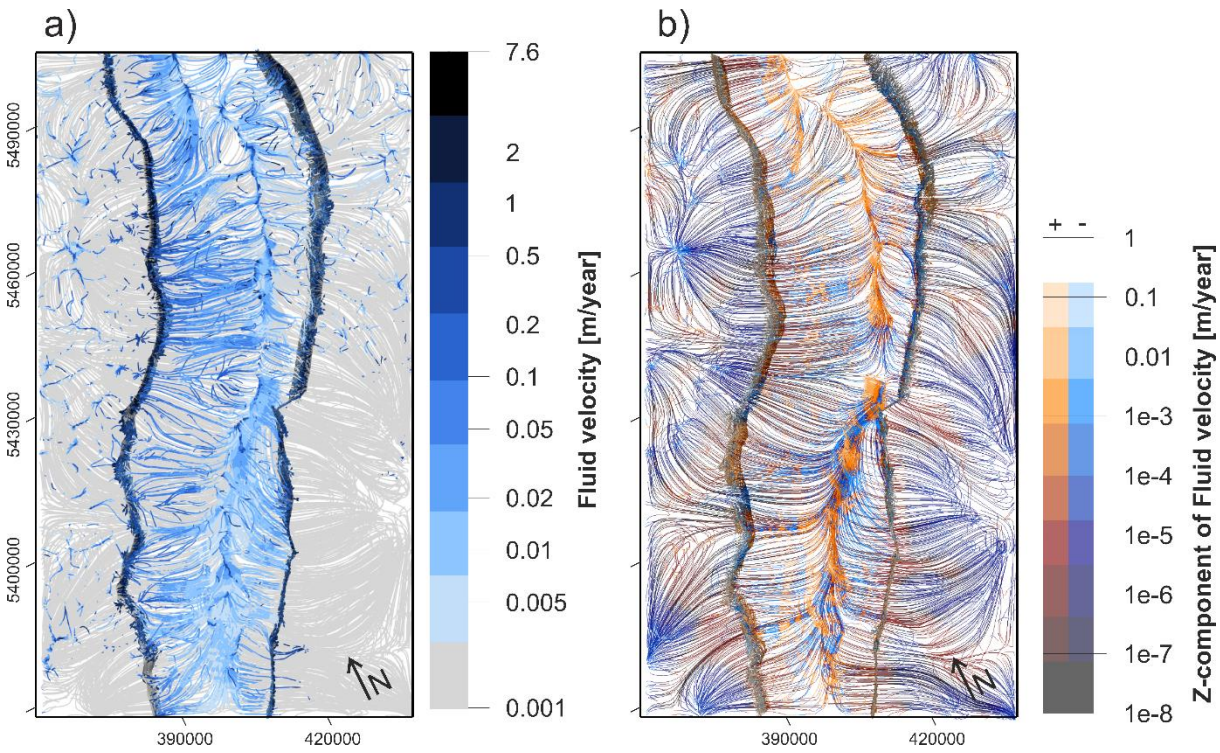

Fig. B4: Hydraulic field of the complex model with illustrated (a) fluid velocities and (b) z-component of the fluid velocity that differentiates the flow into upward (red colours) and downward (blue colours) directed flow averaged for the entire model. Maps are shown in UTM32N and rotated counter-clockwise by approximately 20°.

Table B2: Simulated fluid velocities for each of the geological units of the complex model.

Geological Unit	**Fluid Velocity [m/year]**	
	Min	**Max**
Quaternary	4.2E-3	74
Tertiary	2.5E-4	11
Keuper/Lias/Dogger	3.5E-6	1.3E-1
Muschelkalk	2.3E-4	3.5
Buntsandstein	8.0E-5	2.9
PermoCarboniferous	6.1E-6	3.7E-1
Upper Crust	2.8E-8	4.5E-4
Faults	2.1E-4	9

References

Altherr, R., Holl, A., Hegner, E., Langer, C., Kreuzer, H., 2000. "High-potassium, calc-alkaline I-type plutonism in the European Variscides: northern Vosges (France) and northern Schwarzwald (Germany)." Lithos 50 (1–3), 51-73. doi: 10.1016/S0024-4937(99)00052-3.

Bär, K., 2012. "Untersuchung der tiefengeothermischen Potenziale von Hessen."Dissertation, TU Darmstadt.

Baujard, C., Genter, A., Dalmais, E., Maurer, V., Hehn, R., Rosillette, R., Vidal, J., Schmittbuhl, J., 2017. "Hydrothermal characterization of wells GRT-1 and GRT-2 in Rittershoffen, France: Implications on the understanding of natural flow systems in the rhine graben." Geothermics 65, 255-268. doi: 10.1016/j.geothermics.2016.11.001.

Berger, H.-J., Felix, M., Görne, S., Koch, E., Krentz, O., Förster, A., Förster, H.-J., Konietzky, H., Lunow, C., Walter, K., Schütz, H., Stanek, K., Wagner, S., 2011. "Tiefengeothermie Sachsen." Schriftenreihe des LfULG 9, 1-108.

Clauser, C., Villinger, H., 1990. "Analysis of conductive and convective heat transfer in a sedimentary basin, demonstrated for the Rheingraben." Geophysical Journal International 100 (3), 393-414. doi: 10.1111/j.1365-246X.1990.tb00693.x.

Dezayes, C., Genter, A., Thinon, I., Courrioux, G., Tourlière, B., 2008. "Geothermal potential assessment of clastic Triassic reservoirs (Upper Rhine Graben, France)." PROCEEDINGS, Thirty-Second Workshop on Geothermal Reservoir Engineering Stanford University, Stanford, California, January 28-30, 2008.

Freymark, J., Sippel, J., Scheck-Wenderoth, M., Bär, K., Stiller, M., Fritsche, J.-G., Kracht, M., 2017. "The deep thermal field of the Upper Rhine Graben." Tectonophysics 694, 114-129. doi: 10.1016/j.tecto.2016.11.013.

GeORG-Projektteam, 2013a. "Geopotenziale des tieferen Untergrundes im Oberrheingraben, Fachlich-Technischer Abschlussbericht des INTERREG-Projekts GeORG, Teil 1: Ziele und Ergebnisse des Projekts." LGRB-Informationen 28, 103.

GeORG-Projektteam, 2013b. "Geopotenziale des tieferen Untergrundes im Oberrheingraben, Fachlich-Technischer Abschlussbericht des INTERREG-Projekts GeORG, Teil 2: Geologische Ergebnisse und Nutzungsmöglichkeiten."

GeORG-Projektteam, 2013c. "Geopotenziale des tieferen Untergrundes im Oberrheingraben, Fachlich-Technischer Abschlussbericht des INTERREG-Projekts GeORG, Teil 3: Daten, Methodik, Darstellungsweise."

Guillou-Frottier, L., Carré, C., Bourgine, B., Bouchot, V., Genter, A., 2013. "Structure of hydrothermal convection in the Upper Rhine Graben as inferred from corrected temperature data and basin-scale numerical models." Journal of Volcanology and Geothermal Research 256, 29-49. doi: 10.1016/j.jvolgeores.2013.02.008.

Gutscher, M.-A., 1991. "Gravity interpretation along seismic reflection profile DEKORP 9-N (northern Rhine Graben)." Terra Nova 3 (2), 166-174. doi: 10.1111/j.1365-3121.1991.tb00869.x.

Haenel, R., 1983. "Geothermal Investigations in the Rhenish Massif." In Plateau Uplift: The Rhenish Shield - A Case History, edited by Fuchs, K., Von Gehlen, K., Mälzer, H., Murawski, H., Semmel, A., 228-246. Springer Verlag Berlin, Heidelberg, New York, Tokyo.

Jodocy, M., Stober, I., 2011. "Porositäten und Permeabilitäten im Oberrheingraben und Südwestdeutschen Molassebecken." Erdöl Erdgas Kohle 127(1), 20-27.

Jorand, R., Clauser, C., Marquart, G., Pechnig, R., 2015. "Statistically reliable petrophysical properties of potential reservoir rocks for geothermal energy use and their relation to lithostratigraphy and rock composition: The NE Rhenish Massif and the Lower Rhine Embayment (Germany)." Geothermics 53, 413-428. doi: 10.1016/j.geothermics.2014.08.008.

Krohe, A., Eisbacher, G.H., 1988. "Oblique crustal detachment in the Variscan Schwarzwald, southwestern Germany." Geologische Rundschau 77 (1), 25-43. doi: 10.1007/BF01848674.

Lampe, C., Person, M., 2002. "Advective cooling within sedimentary rift basins - application to the Upper Rhinegraben (Germany)." Marine and Petroleum Geology 19(3), 361-375. doi: 10.1016/S0264-8172(02)00022-3.

Landolt-Börnstein, 1982. "Zahlenwerte und Funktionen aus Naturwissenschaft und Technik". Vol. 1a. Berlin: Springer.

Stein, E., 2001. "The geology of the Odenwald Crystalline Complex." Mineralogy and Petrology 72, 7-28. doi: 10.1007/s007100170024.

Stober, I., Jodocy, M., 2009. "Eigenschaften geothermischer Nutzhorizonte im baden-württembergischen und französischen Teil des Oberrheingrabens." Grundwasser - Zeitschrift der Fachsektion Hydrogeologie 14, 127-137. doi: 10.1007/s00767-009-0103-3.

Stober, I., Bucher, K., 2013. "Geothermal Energy - From Theoretical Models to Exploration and Development." Berlin, Heidelberg: Springer.

Stober, I., Bucher, K., 2015. "Hydraulic and hydrochemical properties of deep sedimentary reservoirs of the Upper Rhine Graben, Europe." Geofluids 15 (3), 464-482. doi: 10.1111/gfl.12122.

Surma, F., Geraud, Y., 2003. "Porosity and Thermal Conductivity of the Soultz-sous-Forêts Granite." In Thermo-Hydro-Mechanical Coupling in Fractured Rock, edited by Kümpel, H.-J., 1125-1136. Birkhäuser Basel.

Wilhelm, H., Berktold, A., Bonjer, K.-P., Jäger, K., Stiefel, A., Strack, K.-M., 1989. "Heat flow, electrical conductivity and seismicity in the Black Forest crust, SW Germany." Geophysical Monograph Series 51. doi: 10.1029/GM051p0215.